NJC

PAPER

View Article Online
View Journal | View Issue

Cite this: *New J. Chem.*, 2019, 43, 1017

Encapsulation of collagenase within biomimetically mineralized metal–organic frameworks: designing biocomposites to prevent collagen degradation†

Odair Bim Júnior, *[a] Ana Bedran-Russo,[b] Jader B. S. Flor,[c] Ana F. S. Borges,[d] Valdecir F. Ximenes,[e] Regina C. G. Frem[c] and Paulo N. Lisboa-Filho[a]

Received 15th October 2018,
Accepted 4th December 2018

DOI: 10.1039/c8nj05246h

rsc.li/njc

A growing class of multifunctional porous materials termed metal–organic frameworks (MOFs) has attracted attention for immobilization of biomolecules *via* self-assembly of inorganic and organic building blocks. Herein, we report the rapid formation of MOF shells surrounding collagen-degrading enzymes by using a biomimetic mineralization approach. Bacterial collagenase, which is functionally related to endogenous proteases in the human body, was used as a nucleating agent to induce the mineralization of zeolitic imidazolate framework-8 (ZIF-8) as a crystalline shell. This zinc-based MOF material was selected due to its remarkable stability under physiological conditions and good biocompatibility. The straightforward, water-based synthesis yielded microporous collagenase-embedded ZIF-8 particles. Once immobilized inside the biomimetically mineralized MOF, the protease presented limited catalytic activity, being ineffective in the proteolysis of a collagen-like peptide. In conclusion, biomimetic mineralization of ZIF-8 using collagenase not only provided immobilization of the enzyme, but also enabled the control of its activity. This synthetic approach provides a potentially useful concept in the prevention of proteolytic activity involved in the degradation of collagen matrices in living organisms.

Introduction

Immobilization of biomolecules on organic–inorganic hybrid materials *via* self-assembly is highly envisaged due to the simple synthetic approach and effective results.[1] A growing class of coordination compounds termed metal–organic frameworks (MOFs) has attracted attention for such a purpose within the last three years.[2] MOFs are porous (mostly microporous) materials constructed through the self-assembly of metal ions and organic linkers.[3,4] MOFs present peculiar properties like high crystallinity and high surface area; besides, their pore networks can serve as a platform for a variety of species, from gases to drugs and biomolecules (*e.g.*, proteins and enzymes).[5–7]

Novel applications of MOFs at the biointerface have shown promising prospects for the protection of biomolecules and control of bioactivity.[8] For instance, recent investigations revealed that large macromolecules like proteins and enzymes are able to induce the formation of protective MOF coatings around them *via* biomimetic mineralization.[9,10] The latter refers to synthetic approaches that mimic fundamental aspects of natural biomineralization, such as the role of a biomolecule (usually a protein) in "templating" the nucleation event and controlling oriented crystal growth.[11] Unlike conventional cargo-loading strategies, in which small guest molecules are infiltrated into the pores of pre-synthesized MOFs, the biomimetic synthesis relies on the *in situ* growth of MOFs at the surface of biomolecules in aqueous media. In essence, the biomimetic mineralization of MOFs enables the generation of porous, crystalline coatings surrounding biomacromolecules, which are commonly much larger than the pore size of most MOF materials.[12]

Protective MOF coatings or shells have been successfully generated using enzymes such as urease, catalase and horseradish peroxidase.[13–15] When integrated with MOFs, enzymes

[a] *UNESP – São Paulo State University, School of Sciences, Department of Physics, Bauru, Brazil. E-mail: odair.bim@unesp.br; Tel: +55 14 3103 6084*
[b] *UIC – University of Illinois at Chicago, College of Dentistry, Department of Restorative Dentistry, Chicago, USA*
[c] *UNESP – São Paulo State University, Institute of Chemistry, Department of Inorganic Chemistry, Araraquara, Brazil*
[d] *USP – University of São Paulo, Bauru School of Dentistry, Department of Operative Dentistry, Endodontics and Dental Materials, Bauru, Brazil*
[e] *UNESP – São Paulo State University, School of Sciences, Department of Chemistry, Bauru, Brazil*

† Electronic supplementary information (ESI) available: Fluorescent labeling of enzymes; calibration curves of collagenase; stability of collagenase in water over time; and pore structure parameters. See DOI: 10.1039/c8nj05246h

tend to be more stable under harsh conditions (*i.e.*, high temperature and aggressive solvents) and present enhanced activity and recyclability; therefore, MOFs have attracted attention as platforms for enzymes for catalytic reactions.[16] On the other hand, MOF shells may also serve as physical barriers to isolate enzymes from their target substrates in situations where catalysis is not desirable.[9] In this case, two criteria are relevant. First, the enzyme needs to be completely enclosed by a protective MOF (*in situ* encapsulation). Second, the enzyme substrate must be larger than the pore aperture of the MOF, so that free substrate molecules are not able to enter the pore network to ultimately complex with the encapsulated enzyme.

Enzyme encapsulation in MOFs – as an approach for controlling enzyme catalysis – could be useful for biomedical applications focused on the prevention of collagen degradation by enzymes such as matrix metalloproteinases (MMPs). Collagen catabolism has an extensive role in physiological and pathological states; hence, the modulation of activity of MMPs (particularly in pathology) has interested scientists for many years.[17,18]

MMPs compose a family of zinc-dependent endogenous proteases that, collectively, are capable of catalyzing the hydrolysis of any type of collagens.[19] Collagens, especially type-I collagen, are the most abundant proteins of the human body, compose specialized forms of extracellular matrices (*e.g.*, bone and tendons) and represent the major barrier to cell migration.[20,21] While collagen catabolism is critical for tissue homeostasis, the excessive activity of MMPs toward collagens has also been implicated in numerous pathological conditions: metastasis,[22] neurodegenerative disorders,[23] osteoporosis,[24] periodontal diseases,[25] *etc.*

The control of collagenolysis in vulnerable situations has traditionally been pursued by means of inhibitors of MMPs.[26] Many inhibitors are compounds that target the active zinc site in the protease to chelate the zinc ion, which is an essential cofactor for activity. Nevertheless, MMP inhibition (as a classic approach) still has not provided satisfactory answers to established problems and presents serious therapeutic limitations (*e.g.*, unwanted side effects resulting from systemic administration due to the lack of MMP specificity).[27]

This work was inspired by the approach of enzyme immobilization – instead of inhibition – as a concept to be better explored for the control of MMP activity. We posited that biocompatible MOFs synthesized *in situ* as crystalline shells for MMPs could prevent the enzymes from catalyzing their reactions. Zeolitic imidazolate framework-8 (ZIF-8), a zinc-based microporous MOF material, was chosen to perform this investigation because it combines the typically attractive features of MOFs with high chemical stability, and can be synthesized under conditions relevant to biomolecules.[9] Besides, ZIF-8 has been deemed biocompatible toward different cell lines and established as a potential candidate for therapeutic applications.[28] The aim of this work was to accomplish the biomimetic mineralization of ZIF-8 using collagenase (from *Clostridium histolyticum*) to immobilize the enzyme within a stable MOF material that could restrain the enzyme's activity.

Experimental

Materials

All chemical reagents, enzymes and enzyme substrates used in the experiments were purchased from Sigma-Aldrich: zinc acetate dihydrate, ≥98% (product 96459, lot BCBT0746); 2-methylimidazole, 99% (product M50850, lot 0000025544); lyophilized collagenase from *Clostridium histolyticum*, activity of 0.25–1.0 FALGPA unit per milligram (product C0130, lot SLBW6959); a collagenase activity colorimetric assay kit (product MAK293, lot SLBX3186); and fluorescein isothiocyanate (product F7250, lot SLBV4791). The products were employed as received without further modifications. The ultrapure water (resistivity of 18.2 MΩ cm) used throughout the experiments was obtained from a Merck Millipore Direct-Q water purification system. To simplify the presentation, *Clostridium histolyticum* collagenase was simply referred to as collagenase, but this enzyme product is composed of a mixture of collagenases with molecular masses ranging from 68 000 to 125 000 Da.

One-pot synthesis of collagenase@ZIF-8 microcrystals

Collagenase was used as a nucleating agent to induce the mineralization of ZIF-8 as crystalline shells. The enzyme encapsulation within the MOF was based on the biomimetic mineralization approach reported by Liang and colleagues,[9] but with modifications as follows. In a small beaker, zinc acetate dihydrate (≈0.11 g, 0.5 mmol) was dissolved in ultrapure water (5 mL) under agitation. In another beaker, 2-methylimidazole (≈ 1.65 g, 20 mmol) was dissolved in ultrapure water (15 mL) and kept under agitation. Approximately 10 mg of lyophilized collagenase was dispersed in the organic ligand solution. Using a Pasteur pipette, the zinc acetate solution was dropped into the ligand solution under constant agitation, causing the system to become turbid almost immediately due to the rapid formation of solid particles. The reaction mixture was stirred for 5 min and then kept at rest for 18 h at room temperature. Subsequently, the obtained precipitate was recovered by centrifugation at 4600*g* for 10 min. The recovered solid particles were purified/washed twice in ultrapure water (15 mL) and ultimately in ethanol (15 mL) by means of sonication and centrifugation cycles. Purification aimed at eliminating acetate ions, residual organic ligands, and collagenase molecules that possibly adsorbed onto the surface of the frameworks. After purification, the biocomposite (collagenase@ZIF-8) was dried for 24 h in a vacuum desiccator. The dry material (nearly 100 mg) was stored in a sealed vial and kept in a refrigerator until taken for the chemical, structural and morphological characterizations.

Synthesis of regular ZIF-8

Regular ZIF-8 crystals were obtained by preparing and mixing aqueous solutions of zinc acetate dihydrate and 2-methylimidazole as described above, except that collagenase was not added to the solutions of precursors. Thus, a regular (not biomimetic) water-based synthesis was conducted, followed by the same steps of purification. Fundamentally, the molar ratio

of zinc salt : ligand : H_2O was 1 : 40 : 2215 in all syntheses, considering ratios used before in the preparation of ZIF-8 in aqueous media.[29]

Chemical and structural characterizations

The synthesized MOF samples were examined by Fourier transform infrared spectroscopy (FTIR) on a Bruker Vertex 70 spectrophotometer. Transmittance spectra were collected from the samples using the following scanning parameters: range, 1400–400 cm^{-1}; resolution, 4 cm^{-1}; and thirty two accumulations. Powder X-ray diffraction (XRD) patterns were collected using a bench diffractometer (MiniFlex 6th generation, Rigaku), employing CuKα1 radiation (λ = 1.5406 Å; 40 kV; 15 mA), in the range of 5–50° at a scan rate of 4° min^{-1} and a step size of 0.04°. The powdered samples were mounted on zero-background sample holders prior to the analysis.

Pore structure and thermal analyses

Pore structure parameters were determined from nitrogen adsorption–desorption measurements carried out on a Micromeritics ASAP 2020 analyzer at 77 K. Samples were degassed under vacuum at 100 °C for 12 h prior to analysis. The surface areas of the materials were determined using the BET (Brunauer–Emmett–Teller) method, and the total pore volumes were calculated as the amount of nitrogen adsorbed at a relative pressure of 0.98. Thermogravimetric analysis (TGA) and differential thermal analysis (DTA) were conducted using a simultaneous thermal analyzer (STA 449 F3 Jupiter, Netzsch). Approximately 10 mg of each sample was placed in 50 μL α-alumina crucibles. TGA-DTA curves were collected using the following parameters: temperature range, 30–1000 °C; heating rate, 10 °C min^{-1}; and flow rate, 50 mL min^{-1} in a dry air atmosphere.

Morphological characterization

The surface morphology of the particles was examined *via* scanning electron microscopy (SEM) on a Zeiss EVO LS15 microscope, operated at an acceleration voltage of 15 kV in a high vacuum mode. Small amounts of MOF samples were re-dispersed in isopropanol and transferred to silicon chip substrates (mounted on stubs using conductive carbon double-sided sticky tape). After complete solvent evaporation, a thin coating of gold was sputtered onto the samples. Transmission electron microscopy (TEM) micrographs were recorded on a Philips CM-200 microscope, operated at 200 kV and using a lanthanum hexaboride (LaB_6) source. Samples were prepared on 200-mesh copper grids covered with carbon films. Confocal laser scanning microscopy (CLSM) was used for examining the presence of dye-labeled collagenase in biomimetically mineralized ZIF-8 particles. The fluorescent labeling of the enzymes using fluorescein isothiocyanate (FITC) and the CLSM analysis are described in the ESI.†

Encapsulation efficiency and triggered release of enzymes

A fresh batch of collagenase@ZIF-8 composites was synthesized. The aqueous phase arising from the biomimetic synthesis was recovered by centrifugation and was analyzed *via* absorption spectroscopy in the ultraviolet-visible (UV-vis) spectral region. Meanwhile, the recovered precipitate was washed twice in water and then re-dispersed in a volume of ultrapure water equivalent to the original supernatant's volume (nearly 22 mL). To trigger the release of enzymes encapsulated within the biomimetically mineralized ZIF-8 crystal, a few drops of concentrated acetic acid were gradually added to the dispersion until the pH was reduced to 5.0 (as monitored with the aid of a digital pH-meter). By decreasing the pH, the dispersion turned into another aqueous phase, since ZIF-8 is markedly unstable in an acidic environment, *i.e.*, the ligand dissociates from the coordination sphere.[30,31] At that point, an aliquot of the aqueous phase was collected and analyzed *via* UV-vis spectroscopy. The spectroscopic data were examined with regard to the presence of collagenase in the aqueous phases, considering that bacterial collagenase showed a distinct absorption band peak at 258 nm, which did not overlap with peaks of other components used in the ZIF-8 synthesis (ESI,† Fig. S2). All liquid samples were transferred to quartz cuvettes for the analysis on a Perkin Elmer Lambda 50 spectrophotometer and ultrapure water was used as a reference in all measurements. To support the UV-vis investigation, complementary experiments were carried out as in the ESI.†

Enzymatic assay

The efficacy of *in situ* mineralized ZIF-8 shells in controlling the collagenase's catalytic activity was verified by means of an enzymatic spectrophotometric assay. The assay involved the use of a synthetic peptide (2-furanacryloyl-leucyl-glycyl-prolyl-alanine or FALGPA) that is hydrolyzed by collagenase in appropriate buffer solution. Collagenase cleaves FALGPA at the leucyl–glycil bond, and the rate of hydrolysis can be typically monitored in terms of a decrease in absorbance at 345 nm.[32,33]

A solution of pure collagenase (1 mg mL^{-1}) and a dispersion of the collagenase@ZIF-8 composite (12 mg mL^{-1}) were prepared in cold ultrapure water for the assay. The composite dispersion contained a total mass of collagenase (encapsulated) comparable to that in the collagenase solution, since the mass percentage of enzymes in the collagenase@ZIF-8 composite had been estimated at 8.5%. Both the collagenase solution and the collagenase@ZIF-8 dispersion were employed to prepare the reaction mixtures for the enzymatic assay as shown in Table 1. The mixtures were prepared in triplicate directly in a 96-well clear plate for immediate analysis on a multi-mode microplate reader (Synergy H1, BioTek). The angular coefficient of the linear region of the obtained curves (absorbance *vs.* time) was adopted to determine the enzyme activity (A) in U mL^{-1} using eqn (1).

$$A = \frac{[(-\mathrm{SLOPE_{SAMPLE}}) - (-\mathrm{SLOPE_{BKG}})] \times V}{V_0 \times 0.53} \quad (1)$$

In eqn (1), V is the total reaction volume in milliliters, V_0 is the volume of the enzyme aliquot in milliliters, and 0.53 is the millimolar extinction coefficient of FALGPA (as informed by the manufacturer in the product's technical bulletin).

Table 1 Reaction mixtures prepared for the enzymatic assay with pure collagenase and the collagenase@ZIF-8 composite

Reaction mixture	Group collagenase	Group collagenase@ZIF-8
Collagenase solution	10 μL	—
Collagenase@ZIF-8 dispersion	—	10 μL
Assay buffer[a]	150 μL	150 μL
Substrate (FALGPA) solution[a]	40 μL	40 μL
Total reaction volume	200 μL	200 μL

[a] The assay buffer and FALGPA solution were obtained from the collagenase assay kit mentioned above. A background (BKG) mixture was prepared for the enzymatic assay by combining 160 μL of assay buffer and 40 μL of FALGPA solution.

Statistical analysis

A one-way analysis of variance (ANOVA) was conducted on enzyme activity, with the enzyme sample (pure collagenase and collagenase@ZIF-8) as an independent variable. The particle size (length) was measured using the software Fiji[34] and the distribution histograms of the particle size were generated using the software OriginPro version 2016.

Results and discussion

Herein, we demonstrate that collagenolytic enzymes can induce the rapid formation of ZIF-8 as crystalline shells in a biomolecule-friendly environment, *i.e.*, aqueous medium, no organic solvent and room temperature. The biomimetic synthesis occurred by simply exposing the target enzyme (bacterial collagenase) to the ZIF-8 precursors (Zn^{2+} ions and 2-methylimidazole) in an aqueous medium (Scheme 1). Important factors for the success of the biomimetic synthesis included but were not limited to the surface chemistry of the biomolecule, the molar ratios of the reactants and their water solubility as this was fundamentally a water-based synthesis.[35,36]

In Fig. 1, the observed XRD pattern of the collagenase@ZIF-8 composite confirmed that the biomimetically mineralized MOF maintained the structural integrity of the as-synthesized ZIF-8. Besides, the very high degree of correspondence between the experimental XRD patterns (red and yellow lines in Fig. 1) and the pattern simulated from ZIF-8 single crystal data also indicated that the experimental materials had the same

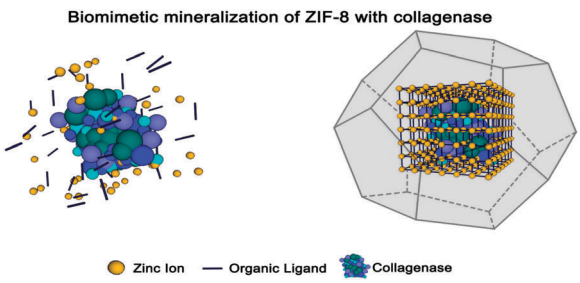

Scheme 1 Schematic model proposing the encapsulation of collagenase *via* biomimetic mineralization of ZIF-8. The biomolecule concentrates the MOF precursors around itself, facilitating the self-assembly of ZIF-8 as a crystalline shell.

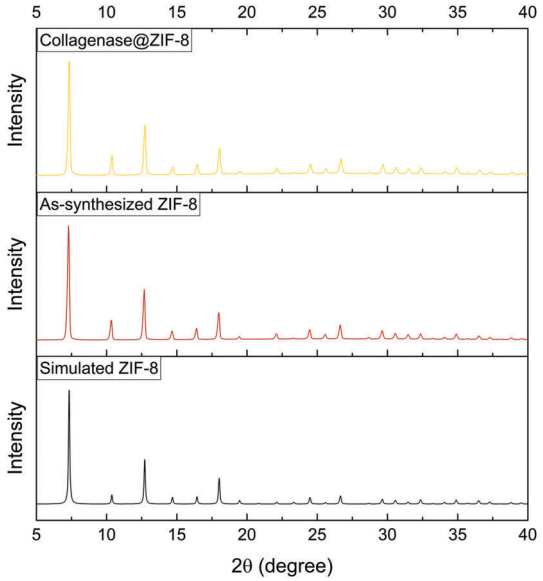

Fig. 1 Simulated XRD pattern from ZIF-8 single crystal data (in black) and experimental XRD patterns of as-synthesized ZIF-8 (in red) and collagenase@ZIF-8 composite (in yellow).

structure as the single crystal. By using the two-theta values of some peaks in the collagenase@ZIF-8 XRD pattern, the lattice parameter was calculated (details in the ESI†) and an average of 17.03 Å ± 0.02 was obtained, which is in accordance with values reported in the literature.[37]

The infrared transmittance spectrum of the as-synthesized ZIF-8 (Fig. 2(a)) was similar to that of the collagenase@ZIF-8 composite (Fig. 2(c)), except that only the latter showed band characteristics of the enzyme, *e.g.*, peaks corresponding to amide I at 1640 cm^{-1} (mainly from C═O stretching) and amide III at 1238 cm^{-1} (Fig. 2(d)).[38] This confirmed the presence of collagenase in the MOF composite, even after the purification/washing steps. To demonstrate that the enzyme was indeed encapsulated within the MOF (instead of adsorbed onto the surface of the framework), a sample of the as-synthesized ZIF-8

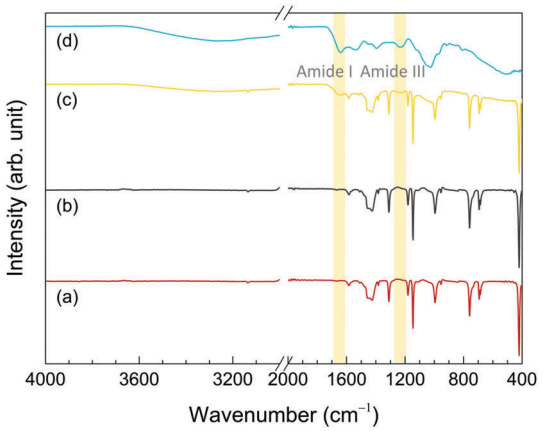

Fig. 2 FTIR spectra of (a) as-synthesized ZIF-8, (b) as-synthesized ZIF-8 posteriorly incubated with collagenase, (c) collagenase@ZIF-8 composite and (d) collagenase.

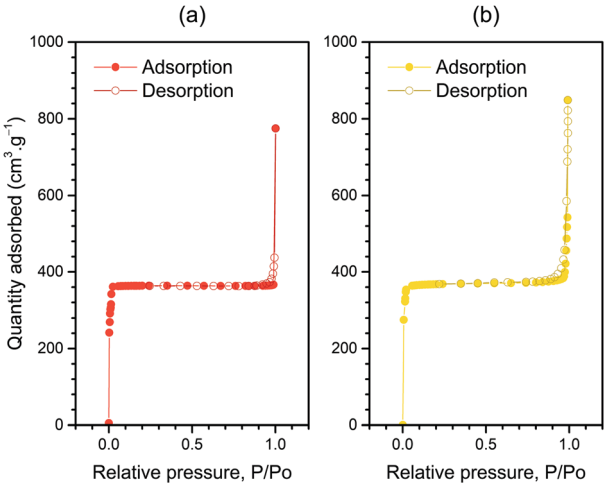

Fig. 3 Nitrogen adsorption–desorption isotherms at 77 K for (a) as-synthesized ZIF-8 and (b) biomimetically mineralized ZIF-8 (collagenase@ZIF-8 composite).

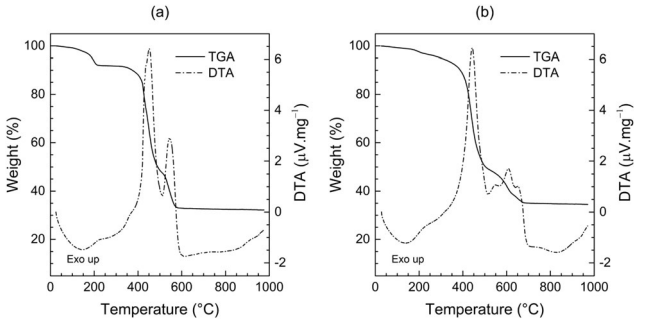

Fig. 4 TGA-DTA curves for (a) as-synthesized ZIF-8 and (b) collagenase@ZIF-8 composite.

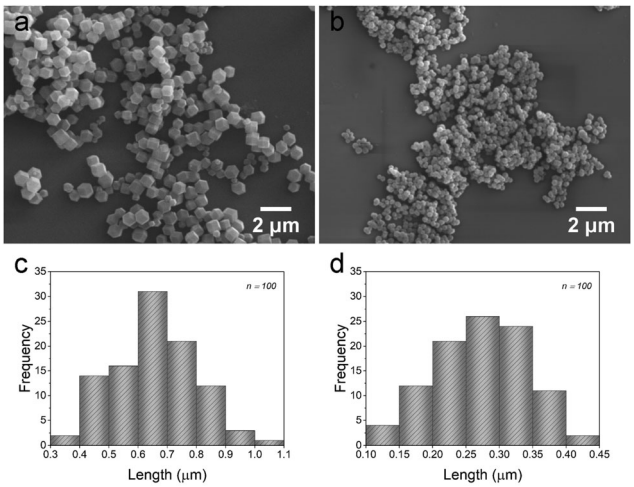

Fig. 5 SEM images for (a) as-synthesized ZIF-8 and (b) collagenase@ZIF-8 composite. Statistical distribution of the particle size: (c) as-synthesized ZIF-8; (d) collagenase@ZIF-8.

was incubated in collagenase solution for 6 h and then submitted to the same thorough washing steps. The infrared spectrum collected from this sample (Fig. 2(b)) did not show the band characteristics of collagenase, reinforcing that the enzyme was embedded in the collagenase@ZIF-8 composite.

Both the as-synthesized and biomimetically mineralized ZIF-8 presented type I adsorption isotherms (Fig. 3), which are commonly given by microporous materials (pore diameter <2 nm) as exemplified by "ZIFs".[39] The obtained materials presented similar total pore volumes (ESI,† Table S2), suggesting that the pores of the biomimetically mineralized MOF shells were not occluded with enzyme molecules. This observation reinforced the assumption that, during the *in situ* encapsulation of the enzyme, the cavities were generated surrounding the entire biomacromolecule, which could not fit directly into a micropore due to its relatively larger size (ESI,† Fig. S4).

The collected TGA-DTA curves are shown in Fig. 4. The first step of weight loss of the as-synthesized ZIF-8 (7.8% up to 215 °C) and the collagenase@ZIF-8 composite (3.2% up to 230 °C) involved endothermic events, probably corresponding to the removal of adsorbed water and unreacted ligands.[40] The decomposition stage of the as-synthesized ZIF-8 started after a plateau in the temperature range of *ca.* 215–335 °C, indicating high thermal stability of the sample. This plateau was not observed in the TGA curve of the collagenase@ZIF-8 composite, possibly due to the gradual degradation of collagenase molecules embedded in the biomimetically mineralized MOF.

SEM micrographs of the MOF materials are shown in Fig. 5. It is possible to observe mostly cuboid shapes for the as-synthesized ZIF-8 (Fig. 5(a)) and smoother shapes for the collagenase@ZIF-8 composite (Fig. 5(b)). Particles of the composite were relatively smaller (0.27 ± 0.07 μm) than regular ZIF-8 (0.66 ± 0.14 μm). Since both materials were prepared using the same molar ratio of Zn^{2+} to ligand (1 : 40) and similar synthetic conditions, the differences in particle size/shape were ascribed to the presence (or absence) of the enzyme in the reaction mixture. In the biomimetic synthesis, the biomolecule's affinity toward the MOF precursors (*i.e.*, metal ions and/or organic ligands) is believed to impel the nucleation/growth of the MOF around the biomolecule.[8,15] Presumably, the amount of collagenase at the beginning of the synthesis (approximately 0.45 mg mL^{-1}) offered too many nucleating sites to a limited amount of ZIF-8 building blocks, in particular, zinc ions. Under such circumstances, the formation of a large number of nuclei and a rapid decrease in the concentration of Zn^{2+} may have resulted in smaller particles. Moreover, the biomolecule (as a mineralization agent) can possibly influence the structural evolution of ZIF-8 over time, which seems to involve the transformation of smaller crystals (metastable phase) into larger ones that are energetically favored.[41]

Evidence of the enzyme encapsulation was first collected from TEM micrographs (Fig. 6). While the as-synthesized ZIF-8 showed well-defined particles with a homogenous density (Fig. 6(a and b)), moderately electron-dense spots could be seen through the collagenase@ZIF-8 composite (Fig. 6(c and d)). Such darker spots were associated with the presence of collagenase or enzyme agglomerates inside the MOF. Convincing evidence of enzyme encapsulation was supported by the CLSM results though (Fig. 7). The fluorescence of FITC-labeled

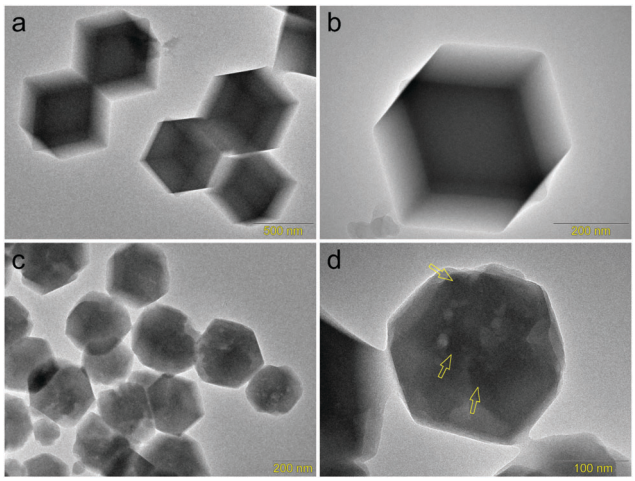

Fig. 6 TEM images of (a and b) as-synthesized ZIF-8 and (c and d) colagenase@ZIF-8 composite. Dark spots indicated by yellow arrows are attributed to the presence of collagenase inside the composite particle.

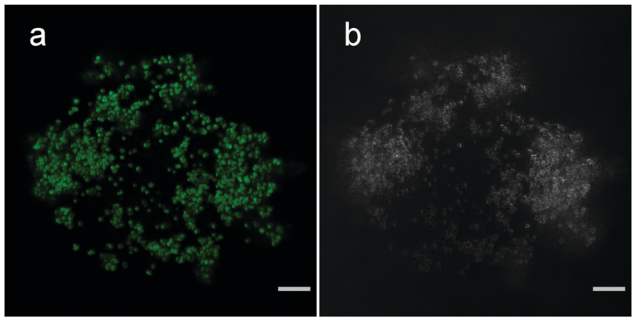

Fig. 7 CLSM images of collagenase@ZIF-8 particles prepared using FITC-labeled collagenase. Images collected in (a) fluorescence mode and (b) transmission mode. Scale bar, 5 μm. Laser excitation wavelength, 488 nm; emission bandwidth, 500–600 nm; ×100/1.4 NA in oil.

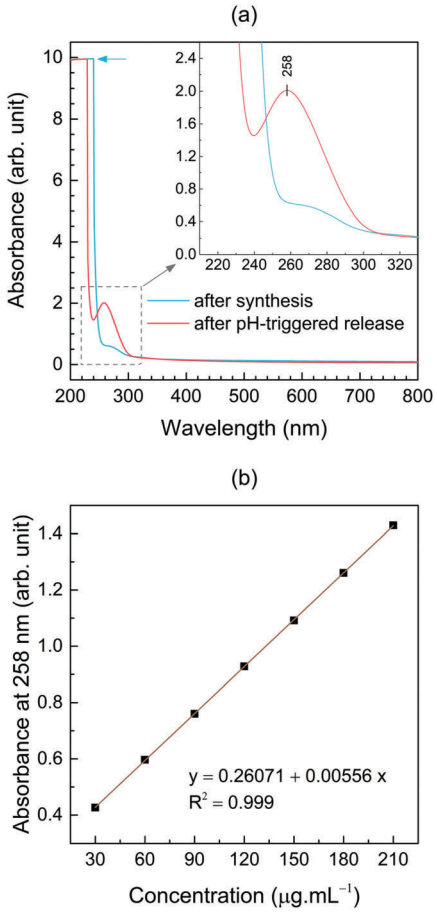

Fig. 8 (a) Absorption spectra of the aqueous phases obtained after the biomimetic synthesis and after the pH-triggered release of collagenase. The blue arrow indicates a saturated band corresponding to the excess of 2-methylimidazole in the solutions. (b) Calibration curve of collagenase in an aqueous solution of 2-methylimidazole.

collagenase inside ZIF-8 shells could clearly be observed upon illumination using a 488 nm laser line, which is suitable for the excitation of fluorescein and its derivatives. The labeling of collagenase using FITC was performed in a separate step prior to using the enzyme in the preparation of the enzyme@MOF sample for the microscopic analysis (ESI†).

The enzyme encapsulation was also verified by analyzing the aqueous phase obtained from both the biomimetic synthesis and the pH-triggered release procedure. After the triggered release procedure, the absorbance at 258 nm (by the enzyme) was three-fold higher compared with that of the supernatant after synthesis (Fig. 8(a)), implying that collagenase had been released from the ZIF-8 shells to the aqueous medium.

The enzyme concentration in the supernatant was determined using a calibration curve of collagenase (Fig. 8(b)), built from UV-vis spectroscopic data. For the calibration curve model, collagenase was dispersed in aqueous solutions containing a large excess of 2-methylimidazole to mimic better the composition of the original supernatant (details in the ESI†). The concentration of collagenase in the supernatant after synthesis was found to be $\approx 68\ \mu g\ mL^{-1}$, which represented about 15% of the initial enzyme concentration in the reaction mixture. Thus, 85% of the total amount of enzyme seemed to be integrated with ZIF-8 during its biomimetic mineralization. The presence of residual collagenase in the supernatant was a sign that the initial enzyme concentration was high enough not to limit the yield of the biomimetic synthesis. If the amount of enzyme in the reaction mixture were not enough, the formation of both regular and biomimetically mineralized ZIF-8 particles would probably have been observed.

In situ mineralized ZIF-8 shells were able to control the activity of collagenase toward FALGPA, a synthetic peptide that mimics part of the primary structure of collagens (Fig. 9). The activity of encapsulated collagenase was extremely low ($0.009 \pm 0.001\ U\ mL^{-1}$), while pure collagenase solution presented an activity about twelve-fold higher ($0.111 \pm 0.004\ U\ mL^{-1}$). The lower activity of the encapsulated enzyme was presumably due to the physical impediment by the MOF, implying that the ZIF-8 shell was an effective barrier to keep the enzyme and the substrate apart. The known crystal structures of *Clostridium* collagenases are typically on a length scale of tens of angstroms (ESI,† Fig. S4), whereas the pore aperture of ZIF-8 is only 3.4 Å.[37]

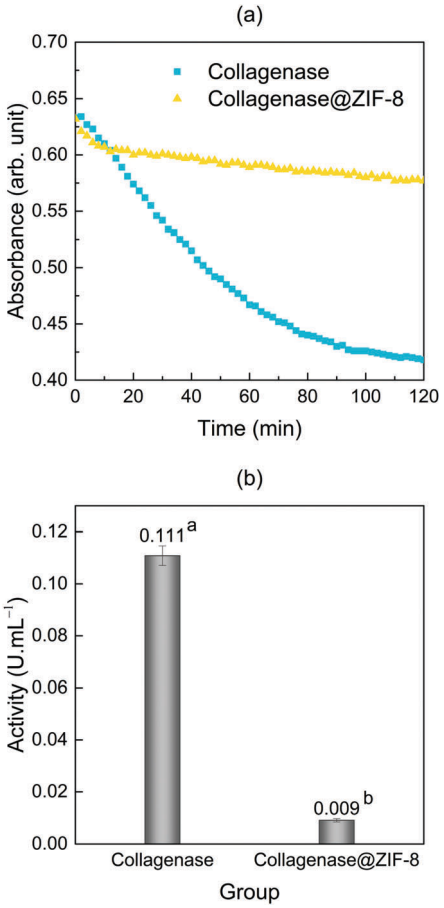

Fig. 9 Enzymatic spectrophotometric assay. (a) Absorbance at 345 nm using FALGPA (an enzyme substrate) over time in the presence of pure collagenase and collagenase@ZIF-8 composite. (b) Catalytic activity of pure collagenase and collagenase@ZIF-8. Different superscript letters indicate that the means were significantly different (p = 0.00; one-way ANOVA conducted with α = 0.05).

Thus, the entrapped collagenase molecules could not leach from the MOF matrix. On the other hand, free FALGPA molecules in the assay mixture were probably unable to enter the ZIF-8 shells. Compared to collagenase, FALGPA is a much smaller molecule (essentially a short sequence of amino acids, Leu–Gly–Pro–Ala),[32] but the size of this peptide should still exceed the pore aperture of ZIF-8. Even if the substrate was small enough to access the ZIF-8 shell and diffuse through the pore framework, the binding to an entrapped enzyme might still depend on other factors, such as the conformational mobility of the enzyme. Quite often, the immobilization of an enzyme in a polymer matrix improves operational stability,[16] but it may also hinder the change in enzyme geometry necessary to achieve an optimal orientation of the catalytic groups for a specific reaction.[42]

Interestingly, the size of the substrate (in relation to the pore apertures and diameters of MOFs) is a key factor to predict how an enzyme@MOF composite should perform: either as a physical barrier or as a platform for a specific catalytic reaction. It is worth saying that, in collagenous tissues, collagens are organized mainly as fibrils with a diameter of about 100 nm.[43] In this sense, the encapsulation of collagenases – or gelatinases and other MMPs – in MOF materials seems to represent an effective approach to isolate these enzymes from their natural collagenous substrates.

Conclusions

In summary, collagenase from *Clostridium histolyticum* was successfully encapsulated in ZIF-8 microcrystals *via* biomimetic mineralization of the MOF, which has been shown to be a facile synthetic approach for protease immobilization. Biomimetically mineralized ZIF-8 shells afforded the control of the enzyme's bioactivity under physiological conditions. Therefore, the immobilization concept addressed here could potentially be useful in the prevention of collagen degradation in organic matrices.

Conflicts of interest

There are no conflicts to declare.

Acknowledgements

We are thankful to the São Paulo Research Foundation (FAPESP, grant # 2018/02186-8) for supporting our research work on the design of MOF biocomposites. We thank Dr Gilbert Bannach and Dr Vera Leopoldo Constantino for providing the use of the STA 449 F3 Jupiter and ASAP 2020 systems respectively. Laboratory assistance provided by Bruna C. Costa, Luciana D. Trino and Mônica Freitas (from CCDPN–SisNano) was greatly appreciated.

References

1 J. Cui and S. Jia, *Coord. Chem. Rev.*, 2017, **352**, 249–263.
2 Z. Lei, C. Gao, L. Chen, Y. He, W. Ma and Z. Lin, *J. Mater. Chem. B*, 2018, **6**, 1581–1594.
3 L. Öhrström, *Crystals*, 2015, **5**, 154–162.
4 R. C. G. Frem, G. Arroyos, G. N. Lucena, J. B. S. Flor, M. A. Fávaro, M. F. Coura and R. C. Alves, *Recent Advances in Complex Functional Materials*, Springer International Publishing, Cham, 2017, pp. 339–369.
5 P. Horcajada, R. Gref, T. Baati, P. K. Allan, G. Maurin, P. Couvreur, G. Férey, R. E. Morris and C. Serre, *Chem. Rev.*, 2012, **112**, 1232–1268.
6 N. Stock and S. Biswas, *Chem. Rev.*, 2012, **112**, 933–969.
7 H. Furukawa, K. E. Cordova, M. O'Keeffe and O. M. Yaghi, *Science*, 2013, **341**, 1230444.
8 C. Doonan, R. Riccò, K. Liang, D. Bradshaw and P. Falcaro, *Acc. Chem. Res.*, 2017, **50**, 1423–1432.
9 K. Liang, R. Ricco, C. M. Doherty, M. J. Styles, S. Bell, N. Kirby, S. Mudie, D. Haylock, A. J. Hill, C. J. Doonan and P. Falcaro, *Nat. Commun.*, 2015, **6**, 7240.
10 Y. Chu, J. Hou, C. Boyer, J. J. Richardson, K. Liang and J. Xu, *Appl. Mater. Today*, 2018, **10**, 93–105.

11 A.-W. Xu, Y. Ma and H. Cölfen, *J. Mater. Chem.*, 2007, **17**, 415–449.
12 J. Zhuang, A. P. Young and C.-K. Tsung, *Small*, 2017, **13**, 1700880.
13 F.-K. Shieh, S.-C. Wang, C.-I. Yen, C.-C. Wu, S. Dutta, L.-Y. Chou, J. V. Morabito, P. Hu, M.-H. Hsu, K. C.-W. Wu and C.-K. Tsung, *J. Am. Chem. Soc.*, 2015, **137**, 4276–4279.
14 K. Liang, C. J. Coghlan, S. G. Bell, C. Doonan and P. Falcaro, *Chem. Commun.*, 2016, **52**, 473–476.
15 X. Wu, C. Yang and J. Ge, *Bioresour. Bioprocess*, 2017, **4**, DOI: 10.1186/s40643-017-0154-8.
16 S. M. F. Vilela and P. Horcajada, *Metal-Organic Frameworks: Applications in Separations and Catalysis*, Wiley-VCH Verlag GmbH & Co. KGaA, Weinheim, Germany, 2018, pp. 447–476.
17 H.-J. Ra and W. C. Parks, *Matrix Biol.*, 2007, **26**, 587–596.
18 S. Amar, L. Smith and G. B. Fields, *Biochim. Biophys. Acta, Mol. Cell Res.*, 2017, **1864**, 1940–1951.
19 L. Campana and J. Iredale, *Stellate Cells in Health and Disease*, Elsevier, 2015, pp. 107–124.
20 M. D. Shoulders and R. T. Raines, *Annu. Rev. Biochem.*, 2009, **78**, 929–958.
21 K. Wolf, S. Alexander, V. Schacht, L. M. Coussens, U. H. von Andrian, J. van Rheenen, E. Deryugina and P. Friedl, *Semin. Cell Dev. Biol.*, 2009, **20**, 931–941.
22 J. Cathcart, A. Pulkoski-Gross and J. Cao, *Genes Dis.*, 2015, **2**, 26–34.
23 B. Mroczko, M. Groblewska and M. Barcikowska, *J. Alzheimer's Dis.*, 2013, **37**, 273–283.
24 K. B. S. Paiva and J. M. Granjeiro, *Prog. Mol. Biol. Transl. Sci.*, 2017, **148**, 203–303.
25 C. Franco, H.-R. Patricia, S. Timo, B. Claudia and H. Marcela, *Int. J. Mol. Sci.*, 2017, **18**, 440.
26 M. Levin, Y. Udi, I. Solomonov and I. Sagi, *Biochim. Biophys. Acta, Mol. Cell Res.*, 2017, **1864**, 1927–1939.
27 A. Winer, S. Adams and P. Mignatti, *Mol. Cancer Ther.*, 2018, **17**, 1147–1155.
28 M. Hoop, C. F. Walde, R. Riccò, F. Mushtaq, A. Terzopoulou, X.-Z. Chen, A. J. DeMello, C. J. Doonan, P. Falcaro, B. J. Nelson, J. Puigmartí-Luis and S. Pané, *Appl. Mater. Today*, 2018, **11**, 13–21.
29 K. Kida, M. Okita, K. Fujita, S. Tanaka and Y. Miyake, *CrystEngComm*, 2013, **15**, 1794–1801.
30 J. Zhuang, C.-H. Kuo, L.-Y. Chou, D.-Y. Liu, E. Weerapana and C.-K. Tsung, *ACS Nano*, 2014, **8**, 2812–2819.
31 X. Wu, C. Yang, J. Ge and Z. Liu, *Nanoscale*, 2015, **7**, 18883–18886.
32 H. E. Van Wart and D. R. Steinbrink, *Anal. Biochem.*, 1981, **113**, 356–365.
33 R. J. Jackson, M. Lien Dao and D. V. Lim, *J. Microbiol. Methods*, 1995, **21**, 209–215.
34 J. Schindelin, I. Arganda-Carreras, E. Frise, V. Kaynig, M. Longair, T. Pietzsch, S. Preibisch, C. Rueden, S. Saalfeld, B. Schmid, J.-Y. Tinevez, D. J. White, V. Hartenstein, K. Eliceiri, P. Tomancak and A. Cardona, *Nat. Methods*, 2012, **9**, 676–682.
35 W. Liang, R. Ricco, N. K. Maddigan, R. P. Dickinson, H. Xu, Q. Li, C. J. Sumby, S. G. Bell, P. Falcaro and C. J. Doonan, *Chem. Mater.*, 2018, **30**, 1069–1077.
36 N. K. Maddigan, A. Tarzia, D. M. Huang, C. J. Sumby, S. G. Bell, P. Falcaro and C. J. Doonan, *Chem. Sci.*, 2018, **9**, 4217–4223.
37 K. S. Park, Z. Ni, A. P. Cote, J. Y. Choi, R. Huang, F. J. Uribe-Romo, H. K. Chae, M. O'Keeffe and O. M. Yaghi, *Proc. Natl. Acad. Sci. U. S. A.*, 2006, **103**, 10186–10191.
38 A. Barth and C. Zscherp, *Q. Rev. Biophys.*, 2002, **35**, 369–430.
39 D. Ongari, P. G. Boyd, S. Barthel, M. Witman, M. Haranczyk and B. Smit, *Langmuir*, 2017, **33**, 14529–14538.
40 X. Wu, J. Ge, C. Yang, M. Hou and Z. Liu, *Chem. Commun.*, 2015, **51**, 13408–13411.
41 S. R. Venna, J. B. Jasinski and M. A. Carreon, *J. Am. Chem. Soc.*, 2010, **132**, 18030–18033.
42 E. T. Denisov, O. M. Sarkisov and G. I. Likhtenshtein, *Chemical Kinetics: Fundamentals and Recent Developments*, Elsevier, Amsterdam, 2003, pp. 502–524.
43 S.-W. Chang and M. J. Buehler, *Mater. Today*, 2014, **17**, 70–76.

